C(s)

Perireceptor and Receptor Events in Olfaction. Comparison of Concentration and Flux Detectors: a Modeling Study

Jean-Pierre Rospars, Vlastimil Křivan[1] and Petr Lánský[2]

Unité de Biométrie, INRA, 78026 Versailles Cedex, France, [1]Institute of Entomology, Academy of Sciences of Czech Republic, Branišovská 31, 370 05 České Budějovice and [2]Institute of Physiology, Academy of Sciences of Czech Republic, Vídeňská 1083, 142 20 Prague 4, Czech Republic

Correspondence to be sent to: Jean-Pierre Rospars, Unité de Biométrie, INRA, 78026 Versailles Cedex, France.
e-mail: rospars@versailles.inra.fr

Abstract

Transduction in chemosensory cells begins with the association of ligand molecules to receptor proteins borne by the cell membrane. The receptor–ligand complexes formed act as signaling compounds that trigger a G-protein cascade. This receptor–ligand interaction, described here by a single-step or double-step reaction, depends on factors controlling the access of the ligand molecules to the cell membrane. Two basic mechanisms can be distinguished: concentration detectors (CD), in which the ligand can freely diffuse to the membrane, and flux detectors (FD), in which it accumulates irreversibly in a distinct perireceptor space where it is chemically deactivated. These two systems, plus their generalization, are investigated and compared. The transient and steady-state numbers of complexes are studied as a function of the external ligand concentration. The biological significance of the results is shown in a well-studied example of FD, the insect sex-pheromone olfactory receptor neuron. How the number of complexes can code for the intensity of stimulation is analyzed using the size, dynamic range and sensitivity of the steady-state responses, and the time needed to reach a predefined level of the transient responses. It is shown that the FD design affords a large increase in sensitivity (a shift of the threshold response towards low concentration) with respect to the CD design, which is paid for by a lesser ability to follow fast changes in stimulus intensity.

Introduction

Olfactory receptor cells are able to transduce chemical stimuli present in their environment into an electrical response [reviewed in (Ronnett and Snyder, 1992; Shepherd, 1992; Lancet and Ben-Arie, 1993; Ache, 1994; Buck, 1996; Schild and Restrepo, 1998); see also (Lauffenburger and Linderman, 1993; Hildebrand and Shepherd, 1997)]. A crucial step in this transduction process is the interaction of the ligand molecules with receptor proteins borne by the cell membrane. Following the ligand–receptor binding and the subsequent receptor activation, a GTP-binding G-protein is activated which in turn acts on enzymes that generate second messengers (e.g. cyclic AMP). These second messengers open a large number of ion channels which change the membrane potential. This response can essentially be regarded as an amplified version of the weak signal resulting from the initial binding.

In our previous work (Lánský and Rospars, 1993, 1995; Rospars *et al.*, 1996a,b) we studied simple models of these transduction events. Concerning ligand–receptor interactions, we considered two basic types of interaction: in the first, the transduction cascade was triggered by mere

binding of the ligand to the receptor to form a complex (single-step interaction); in the second, additionally, an activation of the receptor–ligand complex was required (two-step interaction). The simpler of these two descriptions dates back to Lasareff, who proposed a model in which the effect was proportional to the number of bound receptors at equilibrium state (Lasareff, 1922). Lasareff's model led to several generalizations. Beidler considered a population of different receptors yielding a linear combination of the original characteristics, and also a mixture of different odor ligands (Beidler, 1962). Later, Tateda (Tateda, 1967; Ennis, 1991) suggested that several ligand molecules had to bind to the receptor to activate it. These models were investigated and implemented in a range of different applications (Getz and Akers, 1995; Malaka *et al.*, 1995; Getz, 1999). All of them can be classified as *concentration detectors* (CDs), using the terminology introduced by Kaissling (Kaissling, 1998a), because the sensory membrane is assumed to be directly exposed to the external stimulus.

However, in several systems of interest, the cell membrane is only part of a larger system, so that the ligand–receptor

interaction cannot be considered in isolation (Kaissling, 1974). Ligand molecules, being originally in the external environment, must be transported to the vicinity of the membrane, into the so-called perireceptor space. In insects, for example, olfactory receptor neurons are located within hairs. Odorant molecules are caught on the hairs, diffuse at their surface, enter the hair lumen through small holes in the cuticle and are transported by olfactory binding proteins (Pelosi, 1996) across the lumen to the dendritic membrane of receptor neurons. Because odorant molecules cannot leave the system (Kanaujia and Kaissling, 1985) they must be degraded to prevent their accumulation in the perireceptor space. This involves various enzymatic mechanisms acting on different time scales [slow (Kasang *et al.*, 1988); fast (Ziegelberger, 1995)]. Recently Kaissling, studying olfactory mechanisms in insect sensilla, proposed a model taking into account the perireceptor space and the degradation reactions (Kaissling, 1998a,b). These *flux detectors* (FDs), which offer an elegant solution to the shortcomings of the previous approach (Lánský and Rospars, 1998), might apply to olfactory receptors in both invertebrates and vertebrates.

In the present work we undertake a systematic comparison of the properties of these various perireceptor and receptor models, with the aim of better understanding their signal processing features and, therefore, their biological meaning. We not only consider the CDs and FDs in their pure forms, but also introduce a more general model, denoted GD, that admits the concentration and flux detectors as special cases. For all three detector models, the single- and double-step types of ligand–receptor interactions are studied. Consequently the results obtained can be used for modeling a wide range of chemosensory systems. The relative merits of these models depend on the specific system under examination. For example, CD models are more appropriate for describing systems in which the ligand can relatively freely access and leave the perireceptor space, as seems to be the case in insect carbon dioxide receptors (Stange, 1996), taste receptors, hormone receptor systems and unicellular organisms. FD models can be considered for systems in which the diffusion of the ligand to the perireceptor space is irreversible, as in insect olfactory sensilla. For systems in which the diffusion to and from the perireceptor space is asymmetrical, the more flexible GD model appears as a better choice than the extreme CDs and FDs. Other features differentiating the models from a signal-processing point of view are described and might suggest selecting one of them for further consideration. In all cases single-step models are simpler, which is a good reason to study them because they might give a sufficiently accurate description of some systems. In the present paper, the description is limited to the insect sex-pheromone receptor neuron (we show that CD cannot account for its known properties whereas FD, and its generalized version GFD, can). This is why the analysis of the GD model is not

treated in its full generality. However, the approach followed is intended to be applicable to any chemosensory system.

The response of the model systems to stimuli of various strengths and time courses are analyzed. First, we analyze how the *steady-state* levels of the signaling (bound or activated) complex depend on a stimulation of constant strength. In addition to this steady-state response, we investigate the *kinetics* of the response when the systems are exposed to a stimulus varying in time. We determine and compare the times the systems need to approach equilibria (or to reach any predefined levels) using their response to a stepwise increase of the external stimulus concentration. The square wave stimulation enables us to describe their post-stimulus time evolution and the times they need to return to their resting state. Finally, we also consider periodic stimuli, which are better approximations to natural odorant stimuli than constant ones because, both in air and water, turbulence breaks odor plumes into discontinuous patches (Kramer, 1986; Murlis, 1997). The periodic stimuli allow us to compare the diverse ability of these systems to follow rapidly fluctuating concentrations of ligands. For analyzing the static and dynamic aspects of these responses, we use biologically meaningful characteristics. The static characteristics based on the steady-state conditions include the stimulus concentration at threshold, which measures the *sensitivity* of the system, and the *range* of concentrations discriminated. The time to reach a predefined level (e.g. half-maximum steady-state response) or *latency* is used to characterize the dynamic properties of the systems.

This comparison of various types of detectors is presented in two parts. In the first part (The models and their analytical description) equations describing their behavior are reviewed, and the problems that can and cannot (or not easily) be described analytically are indicated. In the second part (Numerical results), using the analytical results when available or numerical simulations otherwise, the properties of the detectors, including their sensitivity, dynamic range and latency, are compared. The comparisons illustrate the advantages and drawbacks of the CD and FD systems using the moth sex-pheromone olfactory sensillum as a case example, based on the classical investigations by Kaissling and co-workers and on recent numerical estimates of the main parameter values of this system (Kaissling, 1998b).

The models and their analytical description

Stimulations, detectors and receptor–ligand interactions

All symbols used are defined in Table 1. Table 2 gives a synopsis of the six models investigated.

Step, square and periodic stimulations

The ligand molecules L are diluted at time t in the carrier medium (water or air) at a concentration $L_{ex}(t)$. This external concentration can be constant or varying in time in a way that is controllable or at least measurable by an

Table 1   List of symbols and abbreviations

Symbol	Definition	Unit
C	receptor–ligand complex RL; in the simplified model, C is replaced by M	–
C*	activated complex RL; in the simplified model, C* is replaced by M*	–
$C(t)$	concentration of C at time t (dynamic response); see also $M(t)$	µmol/l
$C^*(t)$	concentration of C* at time t (dynamic response); see also $M^*(t)$	µmol/l
CD	concentration detector	–
Δt	time to response, $C(\Delta t) = S$ or $C^*(\Delta t) = S$	s
FD	[pure] flux detector	–
GD	generalized detector (can be CD or FD)	–
GFD	generalized flux detector (more realistic FD)	–
k_1	rate constant of binding reaction R + L → C	µmol/l/s
k_{-1}	rate constant of release reaction C → R + L	s^{-1}
k_2	rate constant of activation reaction C → C*	s^{-1}
k_{-2}	rate constant of deactivation reaction C* → C	s^{-1}
k_i	rate constant of the influx of L in perireceptor space	s^{-1}
k_{-i}	rate constant opposing influx in generalized detector	s^{-1}
k_o	rate constants of the degradation reaction R + L → R + Ł	s^{-1}
L	ligand molecule	–
Ł	degraded ligand molecule	–
L_{ex}	constant concentration of ligand molecules in external space	µmol/l
$L_{ex}(t)$	concentration of ligand molecules in external space at time t	µmol/l
$L(t)$	concentration of ligand in the perireceptor space at time t	µmol/l
$L^M(t)$	concentration of L in perireceptor space at time t for simplified model	µmol/l
λ_0	constant level of periodic stimulation	µmol/l
λ_1	amplitude of periodic stimulation	µmol/l
$M(t)$	concentration of C at time t in simplified model	µmol/l
$M^*(t)$	concentration of C* at time t in simplified model	µmol/l
N	constant concentration of receptors R	µmol/l
ω	angular frequency of periodic stimulation	rad/s
$\phi(t)$	influx to the perireceptor space at time t	µmol/l/s
R	protein receptor in the cell membrane	–
$R(t)$	concentration of free ('non-interacting') receptors at time t	µmol/l
$\overline{R}(t)$	concentration of R bound to L ('interacting') at time t, $N = R(t) + \overline{R}(t)$	µmol/l
S	minimum concentration of C or C* initiating a response	µmol/l
t_0	final instant of stimulation	s
∞	in index, steady-state response	–

experimenter. Four types of stimulation are considered in this article:

Step stimulation. At time $t = 0$ the concentration of the ligand changes abruptly from zero to a constant level L_{ex} and remains at this level (Figure 1a). This stimulation allows one to investigate the steady-state behavior of the system.

Square pulse stimulation. The same change in concentration at time $t = 0$, from zero to level L_{ex}, is followed at $t = t_0$ by an abrupt reset to zero (Figure 1b). It permits one to study the effect of removing the stimulus and the effect of the stimulus duration t_0. The total amount of ligand delivered in this type of stimulation is proportional to $L_{ex}t_0$. The effects of square pulses, either strong and short or weak and long, delivering the same amounts of ligand can be compared.

Periodic stimulations. Two kinds of periodic stimulations were used. The first one (Figure 1c) consists of a series of square pulses with fixed length t_0 and fixed height L_{ex}, which were presented at different frequencies ω (number of pulses per time unit). It has the advantage of being directly comparable to real experimental situations. Unfortunately, in this kind of stimulation changing the frequency also changes the amount of ligand delivered per unit of time. For this reason, we also considered a stimulation described by a sinus wave initiated at time 0 (Figure 2d)

$$L_{ex}(t) = \lambda_0 + \lambda_1 \sin(\omega t) \quad \text{for } t \geq 0 \qquad (1)$$

where the parameters are the angular frequency ω (in rad/s, i.e. the period is $T = 2\pi/\omega$, expressed in s), the amplitude λ_1 and the level of the constant component λ_0 (both in µmol/l). The amplitude λ_1 has to be smaller than or equal to λ_0, so that $L_{ex}(t) \geq 0$. The constant component may be seen as the amount of ligand delivered per unit of time, which is

Table 2 Main models studied (CD, FD, GFD) and their one- and two-step versions[a]

CD1	$L + R \underset{k_{-1}}{\overset{k_1}{\rightleftharpoons}} C$
CD2	$L + R \underset{k_{-1}}{\overset{k_1}{\rightleftharpoons}} C \underset{k_{-2}}{\overset{k_2}{\rightleftharpoons}} C^*$
FD1	$L_{ex} \overset{k_i}{\rightsquigarrow} L, \ L + R \underset{k_{-1}}{\overset{k_1}{\rightleftharpoons}} C \overset{k_o}{\rightarrow} R + Ł$
FD2	$L_{ex} \overset{k_i}{\rightsquigarrow} L, \ L + R \underset{k_{-1}}{\overset{k_1}{\rightleftharpoons}} C \underset{k_{-2}}{\overset{k_2}{\rightleftharpoons}} C^* \overset{k_o}{\rightarrow} R + Ł$
GFD1	$L_{ex} \overset{k_i, \, k_{-i}}{\rightsquigarrow} L, \ L + R \underset{k_{-1}}{\overset{k_1}{\rightleftharpoons}} C \overset{k_o}{\rightarrow} R + Ł$
GFD2	$L_{ex} \overset{k_i, \, k_{-i}}{\rightsquigarrow} L, \ L + R \underset{k_{-1}}{\overset{k_1}{\rightleftharpoons}} C \underset{k_{-2}}{\overset{k_2}{\rightleftharpoons}} C^* \overset{k_o}{\rightarrow} R + Ł$

[a]All symbols are defined in Table 1, except $\rightsquigarrow$, translocation of ligand from external space to perireceptor space; $\rightleftharpoons$, reversible reaction; $\rightarrow$, irreversible reaction.

Figure 1 Ligand concentration $L_{ex}(t)$ in the external medium as a function of time in the four types of stimulation studied, not periodic **(a, b)** and periodic **(c, d)**.

independent of the frequency of stimulation. In the periodic stimulation the main variable of interest is its frequency, which may correspond to some external conditions, e.g. breathing in vertebrate animals or segmentation of the air plume in insects. Stimulation (1) for small t is interesting for studying the transient effects at onset; for large t the solutions converge to a periodic solution (quasi-steady state).

All four stimulation types permit the study of the response of the system at the onset of stimulation, thus solving the problem of initial detection. However, if an organism can detect only concentrations varying in time and loses its ability to perceive a constant stimulus, which is, for example, the case of male moths in a pheromone plume (Kennedy *et al.*, 1980; Willis and Baker, 1984), a periodic stimulation is more appropriate and ω becomes one of the most important parameters.

Concentration, flux and generalized detectors

Ligand molecules L present in the external environment can reach the perireceptor space in the vicinity of the cell sensory membrane. Their concentration there is denoted by $L(t)$. In accordance with Kaissling (Kaissling, 1998a,b), two kinds of transfer between the external space and the perireceptor space are investigated: fast (immediate) and reversible—*concentration detection*—in contrast with slow and irreversible—or *flux detection* (Figure 2).

Concentration detector. This is the classical system in which the odorant concentration $L(t)$ in the perireceptor space is always equal to the concentration L_{ex} in the external space,
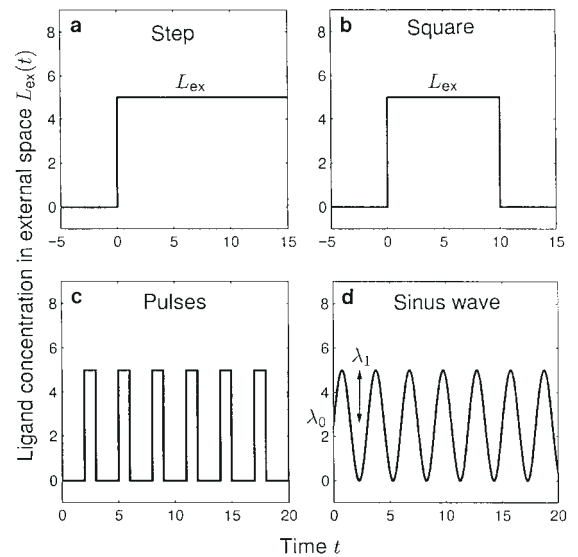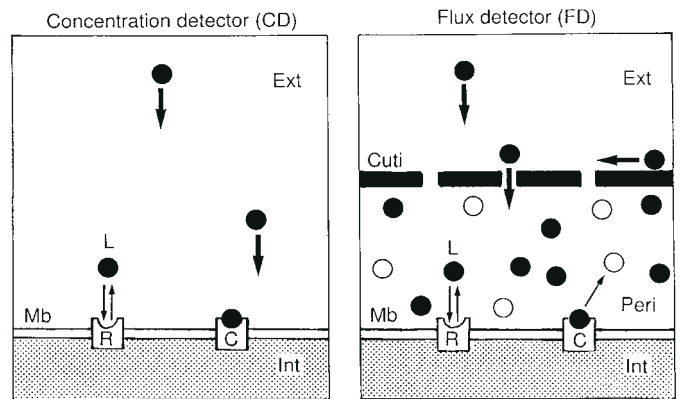

Figure 2 Schematic diagrams of the concentration (CD) and flux (FD) detectors in the case of the single step interaction (CD1 and FD1). In the CD, ligand molecules L (plain circles) in the external medium (Ext) can reach directly and reversibly the cell membrane (Mb) and interact with the receptor protein (R). In the FD, L molecules are collected on a barrier (e.g. cuticle Cuti of an insect sensillum), irreversibly accumulated in the interposed perireceptor space (Peri) and inactivated as molecules Ł (empty circles) that cannot bind with R [redrawn from (Kaissling, 1998a)].

$L(t) = L_{ex}(t)$. The molecules can move freely and instantly between the two spaces, which are therefore indistinguishable. No parameters other than those used for characterizing the receptor–ligand interaction are needed for describing this fast and reversible system (Table 2, CD1 and CD2).

Flux detector. On the contrary, in this system the external and perireceptor spaces are physically distinct and the molecules can move inward only from the first into the second. It follows that the ligand molecules must be degraded in the

perireceptor space to prevent their indefinite accumulation there. The influx in the perireceptor space is

$$\phi(t) = k_i L_{ex}(t) \qquad (2)$$

and the outflow (degradation flux) is $k_o C(t)$ or $k_o C^*(t)$, where $C(t)$ and $C^*(t)$ are the concentrations of the signaling receptor–ligand complex in one- and two-step interactions respectively (see below Single- and double-step ligand interaction with receptors). So, two parameters are needed, the rate constant k_i, characterizing the velocity of the translocation, and the rate constant k_o, characterizing the velocity of the transformation of the ligand molecules L into a degraded form $Ł$ that cannot interact with the receptors (Table 2, FD1 and FD2; note that the arrow $\rightsquigarrow$ denotes a translocation, in contrast to $\rightarrow$, which denotes a chemical reaction).

Generalized detector. However, the two detectors above can be considered as ideal (extreme) cases, whereas many real systems are likely intermediate. Moreover, the FD models can lead to unrealistic consequences if the stimulation is high or the degradation is not sufficient (see below), because the influx to the perireceptor space is independent of the ligand concentration there. This unrealistic behavior can be prevented if the influx $\phi(t)$ slows down when the concentration in the perireceptor space grows. This is the case if it obeys the following kinetics

$$\phi(t) = k_i L_{ex}(t) - k_{-i} L(t) \qquad (3)$$

because the added term $k_{-i} L(t)$, where k_{-i} is a positive constant, increases with $L(t)$, which counterbalances the influx term $k_i L_{ex}(t)$. Equation (3) does not prevent a backward flow of ligand molecules from the perireceptor space if the external concentration decreases and $k_i L_{ex}(t)$ becomes less than $k_{-i} L(t)$. So, the influx of this generalized detector is reversible, as in the pure concentration detector.

A special case of GD, which we call generalized flux detector (GFD), prevents ligand outflow. It obeys the following kinetics

$$\phi(t) = \max(0, k_i L_{ex}(t) - k_{-i} L(t)) \qquad (4)$$

Choosing the maximum of zero and $k_i L_{ex}(t) - k_{-i} L(t)$ prevents a backward flow in the condition stated above. So, the influx of the GFD may be seen as irreversible, like the pure flux detector. This GFD model remains realistic even at high concentrations and, moreover, it behaves at stimulus onset like either the CD or the FD, depending on the values of k_i and k_{-i} (see Generalized flux detector GFD). Only GFD, not GD, is studied in the present paper.

Single- and double-step ligand interaction with receptors

A patch of sensory membrane uniformly covered with identical receptors R is considered (total concentration N). Ligand molecules L can bind to R and create various

complexes. The number of different forms creating the bound class depends on the complexity of the model (Lauffenburger and Linderman, 1993). Here only two forms are considered. In the single-step interaction (Table 2, CD1, FD1 and GFD1), the neuron response is triggered by the binding of the ligand to the receptor, forming a ligand–receptor complex denoted by C. In the double-step interaction (Table 2, CD2, FD2 and GFD2), binding of the ligand is not sufficient to trigger the response; the bound complex must go through an additional step, which can correspond to an allosteric or covalent modification, to produce an activated complex C*. These interactions are characterized by two parameters (rate constants k_1 and k_{-1}; see Table 1) in the single-step case, where k_1 characterizes the velocity of the association between the receptor and ligand and k_{-1} the velocity of the breakdown of the receptor–ligand complex C, and four parameters (rate constants k_1, k_{-1}, k_2 and k_{-2}) in the double-step case, where k_2 characterizes the activation of C in C* and k_{-2} the deactivation of C* in C. The concentrations of C in single-step models and C* in double-step ones are the main variables studied in this paper. Both are referred to as the *signaling complexes*. The time Δt to reach any predefined level S after a stimulation onset, e.g. the concentration S of signaling complexes needed to trigger an action potential, is also studied.

When obtainable, the concise analytical forms describing the evolution in time and steady state of the signaling complex $C(t)$ or $C^*(t)$ are given for the CDs (see Concentration detector CD), FDs (see Flux detector FD) and GFDs (see General flux detector GFD). In all subsections, the special case when L_{ex} is small is studied separately because it is biologically relevant and leads to simpler results. In this case, to avoid any confusion with the exact solutions $C(t)$, the approximated solutions are denoted $M(t)$. Only solutions available in compact form are given here. The details of the mathematical treatment will be published elsewhere (P. Lánský *et al.*, in preparation). For the static CD2, see (Kaissling, 1987; Rospars *et al.*, 1996a,b); for the non-periodic FD1 see (Kaissling, 1998a; Lánský and Rospars, 1998). These solutions are illustrated in Figures 3–6. The parameter values used to draw the curves and the comparisons of the curves are presented in Numerical results.

Concentration detector CD

In CDs the ligand concentrations in the perireceptor space $L(t)$ and in the external space L_{ex} are the same (Figure 3, CD). A natural consequence of this assumption is that $L(t)$ is not influenced by the interaction of L with R, i.e. neither binding to R nor release from R changes the concentration of L.

Model of binding (Table 2, CD1)

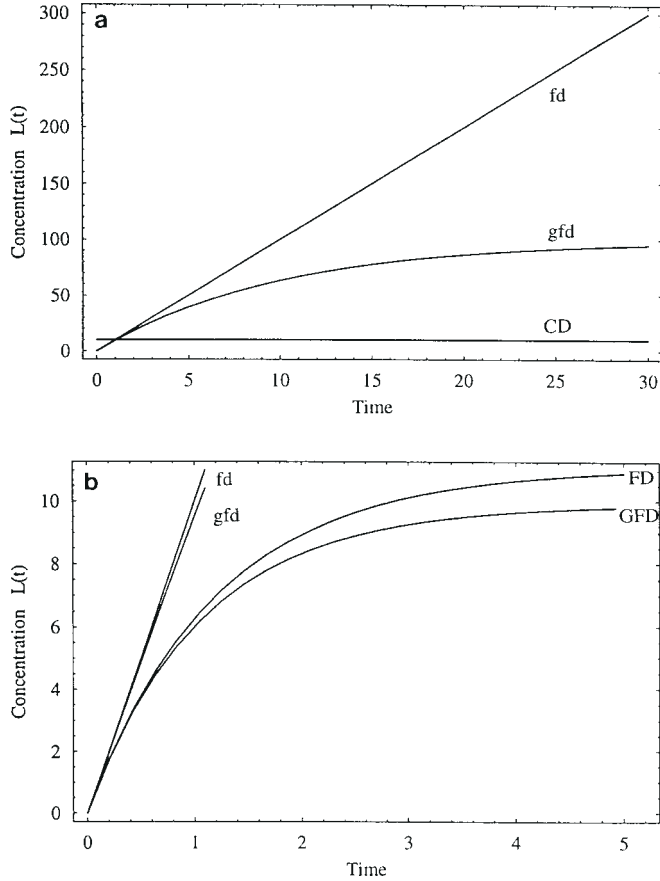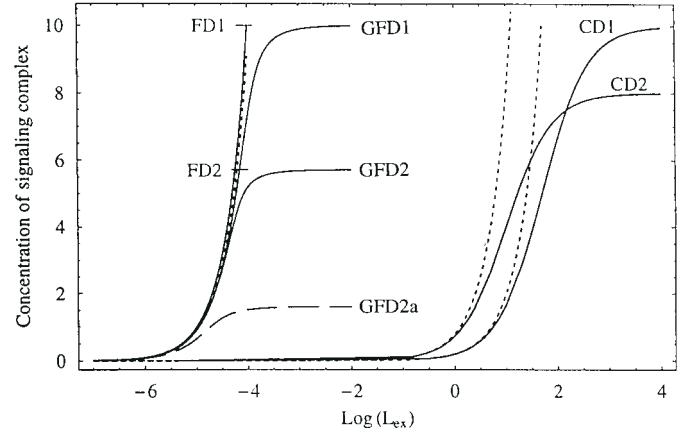The transduction cascade is triggered by mere binding of L

Figure 4 Steady-state concentrations of signaling complex C_∞ for one-step and C^*_∞ for two-step ligand–receptor interactions, as a function of the constant external concentration L_{ex} in a logarithmic scale. Curves for CD models (see Figure 1) are in the right part, curves for FD and GFD models in the left. Dashed curves are low concentration approximations. Curves with horizontal asymptotes $C = N = 10$ (CD1, GFD1) and curves with lower asymptotes are for two-step models (CD2, GFD2). Curves for one- and two-step FD (leftmost) are superimposed and defined only for $L_{ex} < 10^{-4}$ (one-step) and 5.7×10^{-5} µmol/l; the terminal points are indicated by a dash. Parameters: $N = 10$ µmol/l, $k_i = 10^6$ s^{-1}, $k_{-i} = 0.1$ s^{-1}, $k_1 = 0.2$ µmol/s, $k_{-1} = 10$ s^{-1}, $k_2 = 20$ s^{-1}, $k_{-2} = 5$ s^{-1} ($k_2 = 2$s^{-1}, $k_{-2} = 0.5$s^{-1} are presented as GFD2a), $k_o = 10$ s^{-1}.

Figure 3 Concentration $L(t)$ of ligand at the vicinity of receptors following a step stimulation rising at time $t = 0$ from 0 to constant concentration L_{ex}, for different models in the absence ($k_1 = 0$, incomplete model) **(a)** or presence ($k_1 \neq 0$, complete model) **(b)** of receptor–ligand interaction. (a) Horizontal line, concentration detector CD; inclined line, flux detector fd (lowercase indicates incomplete model); exponential curve, generalized flux detector gfd. In fd, $L(t)$ increases indefinitely, in contrast with CD and gfd (asymptote is at $L = 10^2$ µmol/l). In model fd, according to $L(t) = k_i L_{ex} t$, it takes 1 s to reach the level 10 µmol/l, which is reached instantaneously in model CD. This is the main reason for the slower response of FD with respect to CD. In (b), the curves for fd and gfd with $k_1 = 0$ are compared with the complete models ($k_1 \neq 0$, noted FD and GFD). Parameters: in (a), for CD, $L_{ex} = 10$ µmol/l; for fd and gfd, $L_{ex} = 10^{-5}$ µmol/l, $k_i = 10^6$ s^{-1}; for gfd, $k_{-i} = 0.1$ s^{-1}; in (b), for fd and gfd, the parameters are the same as above; for FD and GFD, $N = 10$ µmol/l, $k_1 = 0.2$ µmol/s, $k_{-1} = 10$ s^{-1}, $k_0 = 10$ s^{-1}.
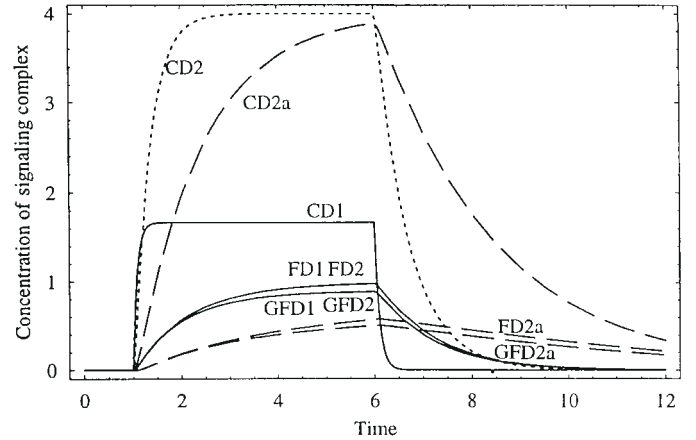

Figure 5 Concentration of signaling complex C_∞ for one-step and C^*_∞ for two-step receptor–ligand interactions, as a function of time for a square wave stimulation. Stimulation is applied from $t = 1$ to $t = 6$ s. The same notations and parameters are used as in Figure 4, except $L_{ex} = 10$ (CD) and 10^{-5} µmol/l (FD and GFD).

to R to form C (complex RL). The time rate of change of C is described by equation (A1) in the Appendix.

Step stimulation. The number $C(t)$ of bound receptor proteins (Figure 4, CD1) rises exponentially from $C(0) = 0$ at time 0 according to

$$C(t) = C_\infty\big(1 - \exp(-t(k_{-1} + k_1 L_{ex}))\big) \tag{5}$$

and reaches a steady-state level C_∞

$$C_\infty = \frac{k_1 L_{ex} N}{k_{-1} + k_1 L_{ex}} \tag{6}$$

The curve C_∞ as a function of L_{ex} is an hyperbola. In the special case when L_{ex} is small, which implies $C_\infty \ll N$, the approximated steady-state level M_∞ of the signaling complex C depends linearly on L_{ex} (Figure 4, dashed line),

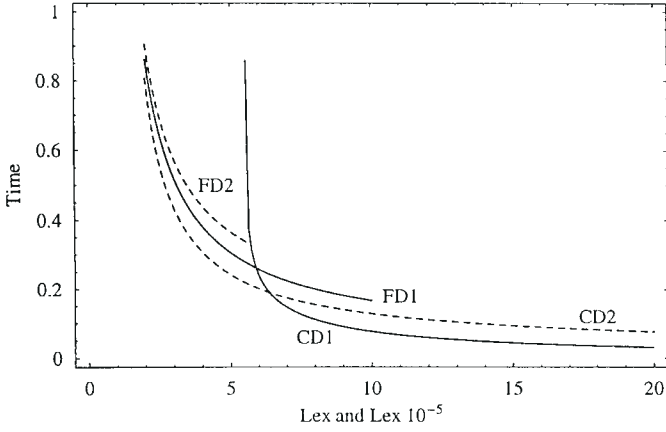$$M_\infty = \frac{k_1 L_{ex} N}{k_{-1}} \tag{7}$$

Figure 6 Time Δt (in s) to reach a predefined concentration S of the signaling complex (C or C^*) as a function of external concentration L_{ex}. The arithmetic scales for CDs (units in µmol/l) and FDs (units in 10^{-5} µmol/l) are different but both extend over ~1 log unit. In the one-step CD model (CD1) Δt tends to zero, whereas in the two-step model (CD2) it tends to a positive horizontal asymptote at 5 ms. FD curves are terminated at saturation of the perireceptor space ($L_{ex} = 10$, $\Delta t = 0.16$ ms for FD1 and 5.7×10^{-5} mol/l, $\Delta t = 0.32$ s for FD2). Vertical asymptotes correspond to concentrations L_{ex} below which the threshold is never reached. Curves for generalized flux detectors GFD (not shown) are practically superimposed on FD1 and FD2 but continue after the saturation points. Parameters: $S = 1$ µmol/l; otherwise they are the same as in Figure 4.

Square stimulation. At the onset of stimulation at time 0, $C(t)$ rises exponentially according to equation (5). After the stimulation that ends at time t_0, the number of signaling complexes decays according to

$$C(t) = C(t_0)\exp(-k_{-1}(t - t_0)) \text{ for } t > t_0 \quad (8)$$

where $C(t)$ is given by equation (5) (Figure 5, CD1). Equations (5) and (8) show that at time t_0 all molecules of ligand are instantly removed ($L_{ex} = 0$) from the vicinity of the membrane. Even the molecules released from the reaction are removed and cannot re-enter it. The time constant $1/(k_{-1} + k_1 L_{ex})$ of the rising phase is always larger than that $1/k_{-1}$ of the decaying phase. So, if $k_{-1} << k_1 L_{ex}$, then the decay is much longer than the rising (Figure 5, CD1) and, after removing the stimulus, it can take a long time to achieve $C(t) = 0$. This feature may be significant if the stimulus is repeated (see below).

If S bound receptors are needed to fire an action potential, then the ligand has to be present at concentration L_{ex} for at least Δt time units. For $S << C_\infty$, with C_∞ given by equation (6), the latency is

$$\Delta t = -\frac{1}{k_{-1} + k_1 L_{ex}}\ln\left(1 - \frac{S}{C_\infty}\right) \approx \frac{S}{k_1 L_{ex} N} \quad (9)$$

The reaction time is inversely proportional to concentration

L_{ex} (Figure 6, CD1). In the low concentration case, the latency

$$\Delta t = -\frac{1}{k_{-1}}\ln\left(1 - \frac{S}{M_\infty}\right) \quad (10)$$

where M_∞ is given by equation (7), is shorter than that given by equation (9).

Periodic stimulation. In the low concentration case the solution after a sufficiently long time is

$$M_\infty(t) = \frac{k_1 N \lambda_0}{k_{-1}} + \frac{k_1 N \lambda_1}{k_{-1}^2 + \omega^2}(k_{-1}\sin\omega t - \omega\cos\omega t) \quad (11)$$

The asymptotic period is $2\pi/\omega$ and the asymptotic amplitude gets to zero proportionally to $1/\omega$, i.e. when the stimulus frequency increases, the response tends to be constant. This means that the system cannot follow very fast time variations of the stimulus, which is a rather intuitive result. For large values of ω the asymptotic levels of constant (equation 7) and periodic (equation 11) stimulations coincide, since in this case M_∞ is the level around which the concentration oscillates very fast with a very small amplitude. In other words, for $\omega \to \infty$, the constant component of stimulation, λ_0, causes the same behavior as $L_{ex} = \lambda_0$ in the step stimulation.

Model of binding and activation (Table 2, CD2)

The receptors may appear in three states: unoccupied R; occupied and not activated C; and occupied and activated C^*. The time rate of change of C and C^* are described by equations (A3) and (A4) in the Appendix.

Step stimulation. This model has often been used for describing odorant–receptor interaction (Kaissling, 1969, 1971; Getz and Akers, 1995; Malaka *et al.*, 1995; Rospars *et al.*, 1996a,b). The kinetics $C^*(t)$ of the activated complex for a step stimulation is given by the sum of two exponentials

$$C^*(t) = C^*_\infty - \frac{C^*_\infty}{\alpha_1 - \alpha_2}(\alpha_1\exp(\alpha_2 t) - \alpha_2\exp(\alpha_1 t)) \quad (12)$$

where α_1 and α_2 can be calculated from the parameters and C^*_∞ is the steady-state level for the signaling complex

$$C^*_\infty = \frac{k_1 L_{ex} N k_2}{k_{-1}k_{-2} + (k_2 + k_{-2})k_1 L_{ex}} \quad (13)$$

So, the hyperbolic dependency of the number of activated receptors on odorant concentration L_{ex} is obtained again as in equation (6) (Figure 4, CD2). However, by manipulating the parameters in equation (13), a larger variability of the

curves can be achieved (Kaissling, 1987; Rospars *et al.*, 1996b). In the low concentration approximation, the steady-state density of activated receptors is again linear (Figure 4, dashed line) as in equation (7)

$$M^*_{\infty} = \frac{k_1 L_{ex} N k_2}{k_{-1} k_{-2}} \qquad (14)$$

Square stimulation. An equation similar to equation (8) can be obtained for the time course of the number of activated receptors after odorant removal in a square wave stimulation (equation 2) (Figure 5, CD2). For the reaction time Δt, after which the threshold S is reached (Figure 6, CD2), the exact analytical solution is not available, but the approximate solution, comparable to equation (9), is

$$\Delta t \approx \sqrt{\frac{2S}{k_1 k_2 L_{ex} N}} \qquad (15)$$

Contrary to CD1, in which the time to reach threshold S tends to zero with increasing L_{ex}, for CD2 there is a minimum time, which can be calculated exactly,

$$\Delta t_{min} = -\frac{1}{k_2 + k_{-2}} \ln\left(1 - \frac{S(k_2 + k_{-2})}{k_2 N}\right) \qquad (16)$$

Periodic stimulation. When the system is stimulated by a periodic signal (equation 1), an analytical solution can be obtained for $M(t)$ and $M_{\infty}(t)$, but it is notationally complicated and will not be given here.

Flux detector FD

The transfer $L_{ex} \overset{k_i}{\leadsto} L$ is unidirectional from outside to inside and compensated by a degradation $C \overset{k_o}{\to} R + Ł$. Consequently, the concentration $L(t)$ of the ligand in the perireceptor space is not the same as the concentration $L_{ex}(t)$ in the external space, but $L(t)$ depends on $L_{ex}(t)$. The differential equations describing this model are given in Appendix A (equations A7–A16).

Model of binding (Table 2, FD1)

Step stimulation. The kinetics $C(t)$ of the activated complex for a step stimulation cannot be given analytically because the corresponding differential equations (A7, A8) are nonlinear. Using these equations with $L_{ex}(t) = L_{ex}$, the steady-state solutions for C and L are

$$C_{\infty} = \frac{k_i L_{ex}}{k_o} \qquad (17)$$

and

$$L_{\infty} = \frac{k_i L_{ex}(k_{-1} + k_o)}{k_1(k_o N - k_i L_{ex})} \qquad (18)$$

under the condition that

$$k_i L_{ex} < k_o N \qquad (19)$$

which means that the influx to the perireceptor space given by equation (2) must be smaller than the maximum possible flow out of it. According to equation (17), the FD1 model does not result in the hyperbolic-like dependency of the receptor response on the external concentration found with the complete CD models, but in a linear dependency similar to that found with the approximate CD models (Figure 4, FD1; compare this curve with the dotted lines for CDs). Of course, for the limiting influx given by equation (19), $L_{ex} \to k_o N/k_i$, the steady-state concentration of ligand in the perireceptor space L_{∞} tends to infinity while C_{∞} tends to N. So, the linearity of FD1 is valid only for a limited range of L_{ex}, and this was also the case for the steady-state approximate CDs (see equation 7 or 14). However, the limits of validity are not the same for CDs and FD1, being based on different reasonings; the validity of approximation (7) is restricted to the values of M_{∞} far below N where few receptors are occupied, $L_{ex} << k_{-1}/k_1$, whereas that of equation (17) is restricted by the fact that C_{∞} cannot exceed N, $L_{ex} < k_0 N/k_i$. Note that the ratio of inward to outward rate constants appears in both relations.

In the low concentration approximation, the asymptotic levels are

$$L^M_{\infty} = \frac{k_i L_{ex}(k_{-1} + k_o)}{k_1 k_o N} \qquad (20)$$

and $M_{\infty} = k_i L_{ex}/k_o$ as in equation (17). It follows from this result that the simplification is less restrictive for the flux detector than for the concentration detector. In a way similar to that of the previous section, we obtain for the simplified model a monotonic growth to an asymptotic level described by two exponentials with negative exponents,

$$M(t) = M_{\infty} - \frac{1}{\alpha_1 - \alpha_2} \times$$
$$((K + M_{\infty}\alpha_1)\exp(\alpha_2 t) - (K + M_{\infty}\alpha_2)\exp(\alpha_1 t)) \qquad (21)$$

where K, α_1 and α_1 can be calculated from the parameters.

Square stimulation. The results for the complete model are available only via numerical techniques. On the other hand, for the simplified model they directly follow from equation (21). Due to the similarity between equations (21) and (12), the approximation (15) for the time to response holds here also. The reaction time Δt, i.e. the time to reach threshold S,

does not tend to zero with increasing strength of stimulation just because the stimulation is limited by equation (19).

Periodic stimulation. For the complete model the asymptotic periodicity and dependency of the amplitude on λ_1 and ω is available only by using the numerical methods. For the simplified low-concentration model the solution is available but notationally complicated.

Model of binding and activation (Table 2, FD2)

Step stimulation. For the step stimulation $L_{ex}(t) = L_{ex}$, the steady-state levels of the stimulus and the signaling complex can be easily obtained from equations (A11)–(A13) in the Appendix:

$$L_\infty = \frac{(k_2 k_o + k_{-1}k_{-2} + k_{-1}k_o)k_i L_{ex}}{\left(Nk_2 k_o - k_i L_{ex}(k_{-2} + k_o + k_2)\right)k_1} \quad (22)$$

$$C^*_\infty = \frac{k_i L_{ex}}{k_o} \quad (23)$$

The formula for L_∞ shows that the condition of saturation of the system is

$$k_i L_{ex} < \frac{Nk_2 k_o}{k_2 + k_{-2} + k_o} \quad (24)$$

It is more restrictive than the condition following from equation (18). On the other hand, if condition (24) is met, the concentration C^*_∞ depends on L_{ex} exactly like C_∞ in equation (17) (Figure 4, FD2); in both cases the concentration of the signaling complex depends only on the parameters related to the influx and degradation. From equation (24), the maximum of C^*_∞ obeys the condition

$$C^*_\infty < \frac{Nk_2}{k_2 + k_{-2} + k_o} \quad (25)$$

For the low-concentration approximation the steady-state levels are unchanged for $M_\infty = C_\infty$ and $M^*_\infty = C^*_\infty$, as given by equation (23) and

$$L^M_\infty = \frac{(k_2 k_o + k_{-1}k_{-2} + k_{-1}k_o)k_i L_{ex}}{Nk_2 k_o k_1} \quad (26)$$

The time courses of L^M, M and M^* can be calculated but the solutions are notationally complicated.

Square and periodic stimulations. No analytical results are available.

Generalized flux detector GFD

In this model the flux $\phi(t)$ depends not only on $L_{ex}(t)$ but also on the concentration inside the perireceptor space $L(t)$, according to relation (4). The differential equations describing this model are (A17)–(A20) in the Appendix. Interestingly, this model behaves like either CD or FD for special values of its parameters, and can also present intermediate features. First, if $k_{-i} \to 0$, $\phi(t)$ reduces to $k_i L_{ex}(t)$, which defines the pure flux detector FD. In this case, the flux is *independent* of concentration $L(t)$ in the perireceptor space, which can rise indefinitely according to equation (18). Second, if k_i is large, $k_i = k_{-i}$ (and $k_o = 0$), and the concentration in the perireceptor space becomes immediately the same as outside when L_{ex} is increased, so that GFD behaves in this case like the pure concentration detector CD (although this is not true when L_{ex} is decreased because of the max condition; see below). Third, for other values of the parameters k_i and k_{-i}, the influx *depends* on $L(t)$. If only the translocation is taken into account and no ligand–receptor interaction takes place, the GFD system is described simply by $dL(t)/dt = \phi(t)$, with $\phi(t)$ given by equation (4). Then, for a constant stimulation, the influx ceases when $L(t)$ increases asymptotically to

$$L_\infty = \frac{k_i}{k_{-i}} L_{ex} \quad (27)$$

(Figure 3, gfd). This example illustrates how the unrealistic behavior of the pure flux model when L_{ex} approaches $k_o N/k_i$ (see equation 24) is removed.

Model of binding (Table 2, GFD1)

Step stimulation. The steady-state values L_∞ and C_∞ are known explicitly; these expressions are relatively long and will not be given here. The dependency of C_∞ on L_{ex} is, for increasing k_{-i}, hyperbolic as the dependencies obtained for CDs (Figure 4, GFD1). Their low-concentration approximations L^M_∞ and M_∞ are simpler expressions

$$M_\infty = \frac{k_1 k_i L_{ex} N}{k_{-i}(k_{-1} + k_o) + k_1 N k_o} \quad (28)$$

and

$$L^M_\infty = \frac{k_i L_{ex}(k_{-1} + k_o)}{k_{-i}(k_{-1} + k_o) + k_1 N k_o} \quad (29)$$

As noticed, for step stimulation, model CD1 can be considered as a special case of the GFD model (equations 20 and 28) assuming $k_o \to 0$ and $k_i \to \infty$. It can be verified that under these two conditions L_∞ tends to L_{ex} and C_∞ is the same as equation (6). Such a comparison cannot be done for the pure flux detection models. For the same intensity of stimulation L_{ex}, the steady-state level of the signaling complex is always lower for GFD (equations 28 and 29) than for FD (equations 17 and 20). Therefore, the model of proportional flux decreases the steady-state concentrations of the reactants obtained for the step stimulation.

Square and periodic stimulations. No analytical results are available.

Model of binding and activation (Table 2, GFD2)

For the step stimulation the equilibria can be calculated but are notationally complex. For the square and periodic stimulations no analytical results are available.

Numerical results

Parameter values

In the following the detectors are compared numerically and graphically, based on the solutions presented above or, when not available, on the numerical solutions of the differential equations given in the Appendix. To make the comparisons easier, the same set of parameter values as given in Table 3 were used throughout. Most of these values were taken from the Kaissling's inspiring study where they are derived from an extensive set of experimental data (Kaissling, 1998b). The parameters were fit to the flux detection model (Kaissling, 1998a) (see above) under the assumptions that the ligand–receptor interaction is a single-step reaction and that the receptor itself catalyzes the oxidation of pheromone molecules into an inactivated form (Ziegelberger, 1995). The measurements, which represent more than two decades of effort [reviewed in (Kaissling, 1986, 1987, 1996)], were performed in the male moth *Antheraea polyphemus* on specialized olfactory receptor neurons that are sensitive to the major component (a 16-carbon acetate) of the sexual pheromone emitted by females. The principles on which the parameter estimation are based are summarized below (a detailed presentation is given in Kaissling, 1998b).

The range of effective pheromone concentration L_{ex} to which the response of the models can be compared is $10^{-12} \leq L_{ex} \leq 10^{-4}$ µmol/l. At the behavioral (Kaissling and Priesner, 1970) and electrophysiological (Zack, 1979) thresholds (10^{-12} µmol/l) there are 300 molecules of pheromone per cm^3 of air and the total uptake is only 15 molecules per antenna in the standard experimental conditions (airflow ~60 cm/s and stimulus duration ~1 s). At the upper end of the range (10^{-4} µmol/l), which corresponds to saturation of the receptor potential, there are 3×10^{10} molecules/cm^3 and the uptake is 1.2×10^5 molecules per hair.

The fictive concentration N of the receptor proteins was expressed with respect to the volume of the hair lumen (~10^{-12} l) (Keil, 1984), under the assumption that they are as tightly packed in the membrane as the rhodopsin molecules in visual cells.

The estimate of the rate constant k_o was based on the assumption that the pheromone degradation reaction saturates for a concentration L_{ex} almost equal to that yielding the maximum electrophysiological response (receptor potential).

The rate constants k_1 and k_{-1} were deduced from the kinetics of the receptor potential (Zack, 1979; Meng *et al.*,

Table 3 Values of parameters used in numerical simulations[a]

Parameter[b]	Main value	Other value[c]
N	10 µmol/l	
k_i	10^6 s^{-1}	
k_{-i}	0.1 s^{-1}	
k_1	0.2 µmol/l/s	
k_{-1}	10 s^{-1}	
k_2	20 s^{-1}	2 s^{-1}
k_{-2}	5 s^{-1}	0.5 s^{-1}
k_o	10 s^{-1}	

[a]Values describing the moth sex-pheromone receptor system.

[b]As defined in Table 1.

[c]Used in Figures 2 and 3.

1989), under the assumption that it is governed primarily by the reversible pheromone–receptor binding reaction. The rate constant k_{-1} of the deactivation reaction was deduced from the decaying phase of the elementary receptor potential, obtained with weak stimulation, which is thought to be triggered by a single pheromone molecule acting on a receptor; k_1 was obtained from the decaying phase of the receptor potential, knowing the other rate constants.

The rate constants for activation k_2 and deactivation k_{-2} of the ligand–receptor complex were not used in Kaissling's studies (Kaissling, 1998a,b) and, to our knowledge, are not known for the pheromone–receptor interaction. We chose a value (0.25) of the deactivation equilibrium constant k_{-2}/k_2 slightly below that (0.5) for which the concentration $L_{0.5}$ at half-maximum steady-state response of the two-step concentration detector is equal to that of the single-step concentration detector, i.e. for which both systems have the same sensitivity. Then, the absolute values of k_2 and k_{-2} were chosen to be in agreement with that of k_o.

The input rate constant k_i was estimated from measurements of the adsorption of radiolabeled pheromone molecules by the antenna (Kanaujia and Kaissling, 1985; Kasang *et al.*, 1988; Kaissling, 1995), knowing the number and volume of the sensory hairs (Gnatzy *et al.*, 1984; Keil, 1984). In (Kaissling, 1998b) the flux $k_i L_{ex}$ is used instead of L_{ex}, so that the value of k_i is not explicitly given. It can be derived from the flux (10^2 µmol/l/s) at saturation of the receptor potential, which leads to $k_i = 10^6$ s^{-1}.

The rate constant k_{-i} limiting the influx in the GFD models was chosen so that the counteracting effect it introduces remains relatively small. Then, the GFD is closer to a FD than to a CD, its response being no different from that of the corresponding FD on most of the L_{ex} scale. With the k_{-i} value chosen (0.1 s^{-1}), according to equation (27), L cannot be greater than $10^7 L_{ex}$. In particular, at the L_{ex} intensity for which L becomes infinite in the pure FD model, L reaches 10^3 µmol/l.

The numerical comparison of the models is divided into

Table 4 Characteristics of the steady-state concentration of the signaling complex

Characteristics	Model[a]					
	CD1	CD2	FD1	FD2	GFD1	GFD2
Magnitude[b] (%)	100	80	100	57.1	100	57.1
Dynamic range[c]						
1–99%	3.99	3.99	1.99	1.99	2.99	2.95
5–95%	2.56	2.56	1.28	1.28	1.71	1.68
Sensitivity[d]						
1%	5.05×10^5	1.01×10^5	1	0.571	1.10	0.622
5%	2.63×10^6	5.26×10^5	5	2.86	5.53	3.12
50%	5×10^7	1×10^7	50	25.6	60	33.6
95%	9.5×10^8	1.9×10^8	95	54.3	285	149
99%	4.95×10^9	9.9×10^8	99	56.6	1089	549

[a]See Tables 1 and 2.

[b]Maximum response for large L_{ex}, expressed as the fraction C_∞/N or C^*_∞/N (in %).

[c]Ratio in log units of concentrations L_{ex} giving magnitudes 99 and 1% (or 95 and 5%).

[d]Concentrations L_{ex} (in pmol/l) giving weak (1, 5%), half (50%) and close to maximum (95, 99%) responses.

three parts with respect to the type of stimulation (step, square wave and periodic). The effect of changing the parameter values, especially the rate constants, is not considered. So, L_{ex} is considered here as the only variable in the system, in accordance with our approach in terms of intensity discrimination. Because only the level of the signaling complex (bound or activated receptors) plays a role in further information transfer, the results for the other compounds are not presented. Comparisons of the simplified (approximation at low concentration) and complete models were performed only in the steady-state case.

Steady-state level of the response

The curves of the concentration of the signaling compound at steady state C_∞ and C_∞^* versus the external concentration L_{ex}, or more appropriately $\log L_{ex}$, depend dramatically on the model considered (Figure 4). From an information coding point of view each of these curves can be characterized by three independent quantities giving the size, dynamic range and sensitivity of the steady-state response (Rospars *et al.*, 1996a,b). The size (vertical dimension) is measured by the maximum steady-state concentration $C_{\infty,max}$ of the signaling complex for large L_{ex}. The dynamic range (horizontal dimension) gives the range of L_{ex} over which the fraction of receptors in the signaling state grows from a small value ε, e.g. 1% of $C_{\infty,max}$, which defines threshold $L_{ex,0.01}$, to almost complete saturation $1 - \varepsilon$, e.g. 99% of $C_{\infty,max}$, which defines saturation $L_{ex,0.99}$. The sensitivity indicates the position of the curve on the horizontal axis L_{ex}, using concentration threshold $L_{ex,0.01}$ or the concentration at half-maximum response $L_{ex,0.5}$. The values of these characteristics are given in Table 4.

The CD models, whether with one- or two-step ligand–

receptor interactions, are characterized by branches of hyperbola that are transformed to logistic curves in log scale. The curves for the GFD models are also sigmoid, whereas those for the one- and two-step FD models are not. As expected from the choice of k_{-i}, FD and GFD curves are superimposed at low concentration and become increasingly different at higher concentration. In this zone, the influence of the influx saturation feature built into GFD becomes dominant and prevents the infinite accumulation of the ligand in the perireceptor space which characterizes FDs when approaching the limiting value $L_{ex,max} = k_o N/k_i = 10^{-4}$ µmol/l (one step; see equation 24) and 0.57×10^{-4} µmol/l (double-step; see equation 23). Beyond this point the system behavior is no longer described by the model [and not merely saturated, as might be wrongly concluded from figure 7 in (Kaissling, 1998b)], although such concentrations can be used experimentally, saturation of air with pheromone being reached only above 1 µmol/l at 20°C.

The most striking feature of Figure 4 is the 6 log units increase in sensitivity afforded by the FD design over the simple CD one, which is seen as a shift of the FD and GFD curves to the left of the CD curves. The shift depends on the value of k_i and consequently on the relative speed of the flying insect with respect to wind. If the relative speed is so low that $k_i = 1$, FD becomes similar to the CD approximation for low concentrations. Then GFD is even closer to CD. So, under this low airspeed condition all models work similarly at steady state.

The maximum *size* of the response depends on the presence or absence of the second (activation) step. In all single-step models the fraction of receptors in the signaling state at large L_{ex} is 100%. This stands in contrast with double-step models, whose asymptotic levels are lower (80%

for CD, 57% for FD and GFD with the parameter values chosen), so that there is no stimulus intensity for which all receptors are activated. Choosing smaller values of k_2 and k_{-2} while keeping their ratio constant would lead to a still smaller maximum (if $k_2 = 2$ and $k_{-2} = 0.5$ s^{-1} it is 16% for FD and GFD). In CD models, the effect of the activation step is to reduce the maximum size of the response and to offer a gain in sensitivity, as the whole curve moves to the left with respect to the single-step reaction curve for $k_2 > k_{-2}$. In contrast, in FDs and GFDs the activation step, when present, entails only a loss in response size without a gain in sensitivity. This can be intuitively justified by the fact that the FD offers the maximum possible sensitivity, which prevents any shift of the GFD response curve to the left.

The *dynamic range* of the CD curves, whether of one or two steps, is 3.99 log units for $\varepsilon = 1\%$ or 2.56 for $\varepsilon = 5\%$, which is a general property of logistic curves. This means that the concentration of signaling receptor complexes increases almost 10 000-fold from threshold, at which 1% of receptors are in the signaling state, to saturation, at which only 1% of receptors remains non-signaling. For FD curves the range is almost 100 times smaller, being 2.00 and 1.28 log units for $\varepsilon = 1$ and 5%, respectively. Finally, the dynamic range for GFD curves is intermediate, of 2.99 and 1.71 log units respectively in the single-step case. Choosing larger values of k_{-i}, that is, increasing the resistance to influx of ligand into the perireceptor space, would widen the dynamic range and be accompanied by a very slight decrease in sensitivity. However, the range of the GFD model can never become greater than that of the CD model.

It follows from their relatively narrow dynamic ranges and their widely distinct sensitivities that the studied examples of CD and FD–GFD work in non-overlapping domains of concentrations. So, the efficiency of one or the other design depends on the natural concentrations of the ligand to be measured.

The low-concentration approximations, for which the solutions are often analytical, are non-sigmoid curves that give reasonable approximations for responses up to 10 or 20% of the maximum response.

Time-course of the response to square wave stimulation

The time-course of the response during stimulus presentation and its decay after stimulus removal can be studied in the case of a square pulse stimulation (Figure 5). Although this is not visible in all cases in Figure 5, the duration of the rising phase is always different from that of the decaying one.

The time Δt needed to achieve any preassigned level S of the response as a function of L_{ex} reflects the response latency in a biologically meaningful way since this time may represent a significant part of the total reaction time of a neuron to stimulation. The Δt versus L_{ex} curves are L-shaped whatever the value of S (Figure 6). In single-step CD and GFD models, Δt goes to zero when L_{ex} is sufficiently large.

In double-step models, Δt tends to a minimum time, which is given for double-step CD by equation (16). For $S = 1$ µmol/l, which is likely to be a relatively large value (10% of N) with respect to the number of activated receptors at maximum response of the neuron, Δt_{min} is 5 ms for CD2 and GFD2, 160 ms for FD1, and 320 ms for FD2.

From an information coding point of view, it is useful to adopt the reverse formulation, i.e. to have fixed L_{ex} and variable S. For each curve, we chose L_{ex} giving a half-maximum response (50% of $C_{\infty,max}$ or $C^*_{\infty,max}$). Then, each curve can be characterized by the time needed to reach a small value ε, e.g. 1% of $C_{\infty,max}$ and almost complete saturation $1 - \varepsilon$, e.g. 99% of $C_{\infty,max}$. These reaction times Δt are given in Table 5. They lead to the following conclusions:

1. CDs and FDs substantially differ in their reaction times. Apart from the steady-state levels already presented above, this is the most obvious difference between them. For example, 95% of the steady-state response is reached in 0.15 s for CD1, 6 s for GFD1 and 8 s for FD1. So, the CD's detector follows the square wave with minimum distortion, whereas the responses of FDs and GFDs rise and decay more slowly, introducing a noticeable distortion. This means that there is a trade-off between the large increase in sensitivity provided by the FD design and the significant decrease in its capacity to reflect reliably the rapid fluctuations of the signal.
2. For low response levels ($\varepsilon < 50\%$) double-step models are slower than their single-step counterparts. The difference is striking for CDs, the reaction time being 1 ms for CD1 and 16 ms for CD2 at $\varepsilon = 1\%$; it is lesser for FDs and GFDs, ~30 ms for one step and 60 ms for two steps. However, for relative levels above 50%, FD2 and GFD2 become slightly faster than their counterparts FD1 and GFD1.
3. For very low response levels, which are significant for stimulus detection (see Discussion), the response times can become very short also for FDs and GFDs. For example, with L_{ex} eliciting a half-maximum response and $\varepsilon = 10^{-5}$ (~10^{-4} µmol/l for the signaling complex), the reaction times predicted by the models are in the 1–5 ms range. This is a very short time compared with transduction time, suggesting that the perireceptor and receptor events are not the limiting steps in the odorant detection process.

Time-course of the response to periodic stimulation

The temporal features of the response observable with square-wave stimulations are emphasized in the case of stimulations with periodic intensity. For all types of detectors the frequency and amplitude of the stimulus must be considered simultaneously.

All systems achieve, after a certain delay, a periodic response which follows the stimulus with the same period. The level around which the response is modulated is the

Table 5 Times (in ms) to reach preassigned levels[a] for fixed stimulus intensity[b]

Levels ε	Model[c]					
	CD1	CD2	FD1	FD2	GFD1	GFD2
Very low						
10^{-5}	<1	<1	1	5	1	5
10^{-4}	<1	1	3	12	3	11
10^{-3}	<1	5	10	27	9	26
Low						
1%	1	16	36	67	32	63
5%	3	39	97	143	86	132
Middle						
50%	35	267	1033	986	843	836
High						
95%	150	1051	7826	6977	5897	5439
99%	230	1599	1.4×10^5	1.2×10^5	1.0×10^5	9560

[a]Preassigned levels defined as $S = \varepsilon C_\infty$ or $S = \varepsilon C^*_\infty$.

[b]Stimulus concentration L_{ex} giving half-maximum response (magnitude $\times$ 0.5; see Table 3).

[c]See Tables 1 and 2.

steady-state level observed under constant stimulation. Since the CD models are fast responding, the periodic regime is achieved more quickly than in the FD and GFD models.

For sufficiently low frequency, the amplitude of the response approaches a maximum which is equal to the level that would be achieved by a constant stimulation $L_{ex} = \lambda_0 + \lambda_1$. With increasing frequency, the response, although still periodic, does not reproduce the upper and lower parts of the signal, so that the amplitude of the oscillating part of the response decreases. Finally, the system averages almost completely the quickly alternating signal which evokes a practically constant response. Figures 7 and 8 show that the amplitude of the response decreases at a slower rate for CDs than for FDs. When the frequency increases from 1 to 10 Hz, the amplitude decreases by 20% from 0.64 to 0.5 µmol/l for single-step CD, less than four times from 0.76 to 0.24 for double-step CD, and more than five times from 0.22 to 0.03 for single- and double-step FDs and GFDs. Although the same qualitative behaviors with roughly three domains (periodic with large amplitude, periodic with small amplitude, non-periodic) can be observed for both detector types, the dependency of these domains on stimulus frequency are quite different. Similarly, as seen in Figure 7, the phase shift with respect to the stimulation is larger for slowly responding systems.

Figure 9 illustrates the response of the model to the periodic stimulation with square pulses as used in actual experiments (see Discussion for details). It shows clearly the effect of periodicity, although in this kind of stimulation the amount of ligand delivered per unit of time is changed when the frequency changes. The ratio of the amplitude of the periodic part of the signal to its mean constant level falls from 69% at 1 Hz to 15% at 3 Hz and 2% at 10 Hz.

Discussion

Concentration and flux detectors

The distinction between concentration and flux chemosensory detectors has been recently proposed by Kaissling (Kaissling, 1998a). It puts the conditions in which chemosensory systems operate in a new light and is of major importance in understanding their design principles. The significance of these concepts is illustrated here by comparing three models, the concentration detector (CD), the pure flux detector (FD) and the generalized flux detector (GFD). Each of these models was studied at two levels of complexity, the subsequent transduction cascade being triggered either by mere binding of the ligand to the receptor, in a single step, or by binding plus activation, in two steps.

The CD models are described by only three (single step: k_1, k_{-1} and N; see Table 1) or five (double step: as for single step, but adding k_2 and k_{-2}) parameters in their versions studied here, which involve only ligand–receptor interactions and no ligand-degrading reaction. In such systems, the signaling receptor complex responds directly to the external ligand concentration. The models apply to chemosensory membranes that are almost directly exposed to their environment, as might be the case for taste receptors, insect carbon dioxide receptors (Stange, 1996), hormone receptor systems and unicellular organisms.

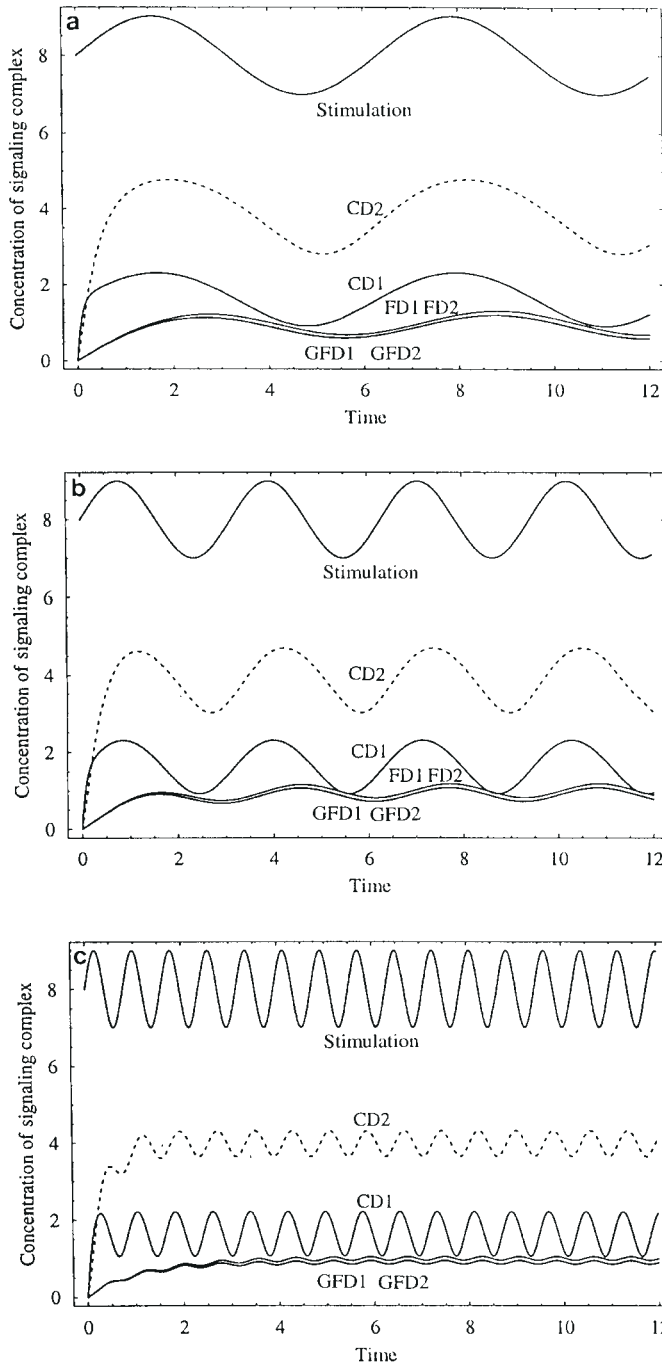The flux detectors, in either their original (FD) or

Figure 7 Concentration of signaling complex *C* for one-step and *C** for two-step ligand–receptor interactions, as a function of time for periodic stimulations of different frequencies ω. Stimulations are $L_{ex}(t) = 10(1 + 0.5\sin\omega t)$ (CD1 and CD2) and $10^{-5}(1 + 0.5\sin\omega t)$ μmol/l (FD and GFD), with ω = 1 s^{-1} **(a)**, ω = 2 s^{-1} **(b)** and ω = 8 s^{-1} **(c)**. Curves FD1 and FD2 are superimposed, as are curves GFD1 and GFD2. $L_{ex}(t)$ is shown schematically at the top of each frame (Stimulation). The same notations and parameters as in Figure 4 are used, except for $L_{ex}(t)$.
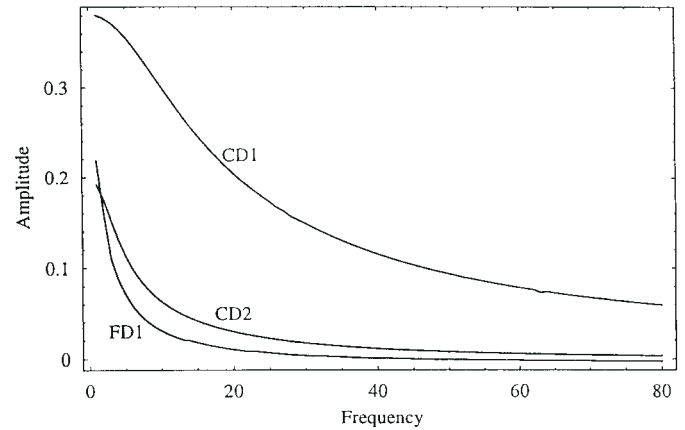

Figure 8 Relative amplitude of response as a function of frequency ω of stimulation. The amplitude is half the distance between two successive extremes (one-half period apart) of concentrations of signaling complex *C* for one-step and *C** for two-step ligand–receptor interactions. The same notations and parameters are used as in Figure 7.

ligand molecules in the perireceptor space and, on the other hand, the symmetric degradation reaction (k_o) responsible for their deactivation. They apply to chemosensory systems that collect the ligand of interest in a periplasmic space using, for example, either binding proteins attached to the membrane, a mucus layer or a physical barrier. Therefore, any chemosensory cell might belong to this category, and most odorant receptor systems probably belong to it.

Some models can be transformed to another by selecting appropriate reaction rate constants. For $k_2 = 0$, the models with a two-step reaction simplify into the models with a one-step reaction. For large k_i, $k_i = k_{-i}$ and $k_o = 0$, GFDs, but not FDs, are transformed into CDs. However, this is true only at stimulation onset because ligand outflow is not permitted in GFDs, so that at offset their behavior is different from that of CDs. The condition $k_o = 0$ is needed in the present form of the CD models; however, this is only a formal change because the degradation reaction governed by k_o might have been included also in the CD models. Note that this degradation mechanism has been kept as simple as possible, the receptor acting as an enzyme. A separate enzyme may be also considered; its effect in FD is to change both steady-state curves shown in Figure 4 in sigmoid curves [see figure 7 in (Kaissling 1998a)] and the time-course of the signaling complex.

The equations can be linearized for $L_{ex}(t)$ small enough, i.e. for a number of signaling complex C or C* much smaller than the total number of receptors. This low-concentration situation is often met in reality (see the last section of this paper) and is probably the only physiologically meaningful one (Rospars *et al.*, 2000). Otherwise full non-linear versions must be considered.
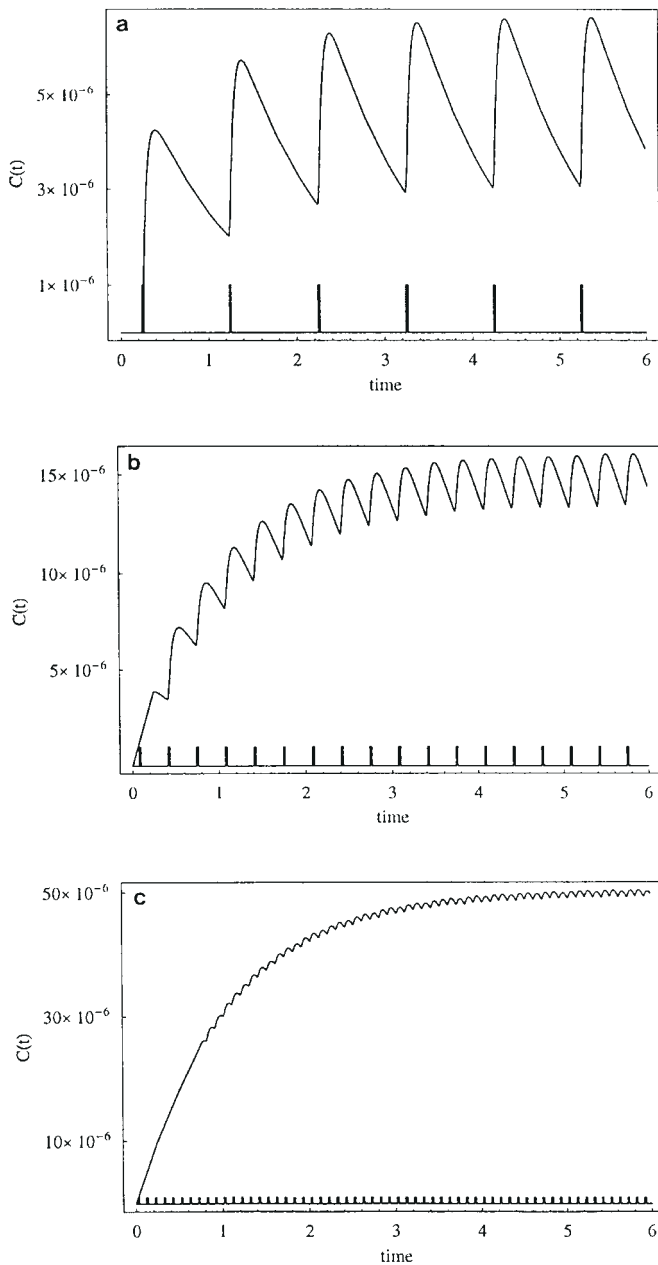
modified (GFD) form, involve two or three more para-meters that describe, on one hand, the adsorption process (k_i in FD, k_i and k_{-i} in GFD) responsible for accumulating

Figure 9 Concentration of signaling complex C for one-step ligand–receptor interactions as a function of time for periodic square-pulsed stimulations at different frequencies $\omega = 1$ **(a)**, 3 **(b)** and 10 **(c)** Hz. Parameters are as in Figure 4, except $L_{ex} = 2.5 \times 10^{-9}$ μmol/l and pulse duration $t_0 = 20$ ms.

Comparison of concentration and flux detectors in the case of moth olfaction

The behavior of the various detector models has been illustrated in the special case of the reception of sexual pheromone by moths, as originally studied by Kaissling. The most basic conclusion resulting from this illustration is that, using the parameter values that describe the actual system (as given in Table 3), the high sensitivity of the

system cannot be accounted for by a concentration detector, which falls short by six orders of magnitude. Only a flux detector can account for this high sensitivity. Now, the relative merits for describing the system of the different versions of flux detectors, the original FD or its generalized version GFD, whether one step or two, must be assessed on other grounds. The two-step versions, having two more parameters than single-step versions, are more flexible. The same is true for the GFD version, which has one more parameter than FD (k_{-i}) and thus can fit experimental data more precisely and, moreover, can describe any intermediate detector between the two extremes that are CDs and FDs.

Now it can be instructive to adopt an engineering point of view on this system and to wonder why sex-pheromone reception is not based on a CD device. This question arises because it is *a priori* possible to design a CD which is sensitive enough to monitor the sex-pheromone concentration range actually observed. Consider, for example, the steady-state response of the single-step CD. The problem to solve consists in shifting the CD1 curve as shown in Figure 4 to the left by 6 log units so that it coincides approximately with the FD1–GFD1 curves. This can be done if the dissociation equilibrium constant k_{-1}/k_1, which gives the ligand concentration at half-maximum response, is multiplied by 10^{-6}, i.e. from its actual value of 5×10^{-5} mol/l (see Table 3) to 5×10^{-11} mol/l. This corresponds to a shift from the low-affinity end to the high-affinity end of the various known receptors (Lauffenburger and Linderman, 1993). So, the idea of a sex-pheromone CD does not appear unrealistic as far as the receptor-ligand is concerned.

So, the reason why the actual sex-pheromone system is a flux detector must be found elsewhere. A possible interpretation is that the flux-detector design is the only one compatible with the lipophilic nature of the bombykol molecules, which sticks them to the cuticle, and the multiporous cuticular structure, which entails irreversible entrance into the perireceptor space. Both features preclude free return of the ligand to air as in the (ideal) case of the CD. Then the low affinity of the receptor to its ligand would be a secondary adaptation. It is such that it permits monitoring the actual concentration range of bombykol, given the unavoidable accumulation of these molecules in the vicinity of the receptors. So, contrary to what might be thought *a priori*, the affinity of the receptors to bombykol would not be a limiting factor for the global sensitivity of the system.

Properties of flux detectors in the case of moth olfaction

The parameter values used in Table 3, which describe the sex-pheromone receptor system, can be changed in relatively large ranges without altering the qualitative conclusions presented. For example, the input rate constant k_i influences the magnitude of the gain in sensity to concentration and the corresponding gain in temporal acuity, afforded by FDs (including GFDs) with respect to CDs. Only the magnitude, not the existence of these two effects of relative gain in

sensitivity and time resolution, which are the major properties of the systems from the signal processing point of view we adopt here, can be influenced by manipulating the value of k_i. These are structural features of the models that are insensitive to the values of the parameters. Unfortunately, the exact value of k_i cannot be easily determined experimentally because the perireceptor space, which is the volume in which the pheromone molecules have easy access to the receptors, is not well defined. If the whole internal hair volume were considered as the actual perireceptor space, which corresponds to a perireceptor layer ~1 μm thick, a lower bound of $k_i = 1.5 \times 10^{-4}$ s^{-1} would hold. Then, according to equation (17), i.e. assuming the one-step FD model gives a correct description, and using $k_o = 10$ s^{-1}, one finds that at the stimulus intensity giving the maximum value of the steady-state receptor potential ($L_{ex} = 10^{-4}$ μmol/l), only 1.5% of the receptors are bound to pheromone molecules. Another possible assumption (but unlikely to be correct) (Rospars *et al.*, 2000) is that all receptors are occupied ($C_\infty = N = 10$ μmol/l) for $L_{ex} = 10^{-4}$ μmol/l. Then, one finds from equation (17) that $k_i = 10^6$ s^{-1}, corresponding to a perireceptor layer only 0.2 μm thick.

The long time constant of flux detectors suggests that the steady-state level is not of primary importance in intensity coding. One possibility is that these systems are not primarily working as sensors of stimulus intensity with graded response, but as sensors of stimulus presence with binary (yes or no) response. Indeed, if the spiking threshold is low enough, which is actually the case in the moth sexual pheromone receptor neuron, it is crossed with very small latency (see Table 5), so that spike firing can reliably follow the fast temporal variations of the signal even if the steady-state level of the signaling receptor complex (and consequently the receptor potential) cannot. For example, a moth flying through a pheromone plume subdivided into small clumps of molecules would never stay long enough in a clump to measure its concentration, which might even be meaningless in this case. However, without considering such an extreme case, another possibility of fast measurement of odor intensity is possible based on the slope of the dynamic response (signaling complex or receptor potential) with respect to time. This is a straightforward interpretation of Figure 6, which represents an expression of the slope $S/\Delta t$ via time Δt needed to reach a constant predefined level S. The regular decrease of Δt as a function of L_{ex} shows that it can provide a reliable measure of L_{ex}. This hypothetic mechanism would call for a spike generating mechanism in which the first spike would signal the onset of the stimulation and the subsequent interspike intervals would allow the system to estimate L_{ex} via Δt.

In the models studied the dynamic range 1–99% never exceeds 4 log units (CD1) and it can be as narrow as 2 (FD1) (see Table 4). This stands in contrast with the >8 log-unit range of the receptor potential (Zack, 1979) under the same conditions. Consequently, the difference must be accounted for by the transduction cascade and the conductance-to-voltage conversion. The latter conversion can account for part of the widening effect, provided there is a long enough single sensory dendrite and a small input resistance of the non-sensory part of the neuron, especially a large soma (Vermeulen and Rospars, 1998), a situation that is reminiscent of the sex-pheromone receptor neuron. In this case the dynamic range of the receptor potential is always >4 (Rospars *et al.*, 1996a,b).

The lower region of the range is the most important in practice. The conventional threshold defined by $\varepsilon = 1\%$ corresponds to a concentration of 0.1 μmol/l of the signaling complex, i.e. 1.6×10^5 molecules per dendrite. This is a large number since a single complex, which corresponds to a concentration of 6.3×10^{-7} μmol/l (with the values selected in Table 3), is sufficient to elicit a spike (Kaissling and Priesner, 1970; Kaissling, 1971). What is the stimulus intensity which elicits this picomolar concentration of C or C^*? Since all FD and GFD models have the same behavior at low L_{ex} concentration, equation (17) can be used to calculate this extreme threshold. One finds $L_{ex} \approx 10^{-11}$ μmol/l, which is in good agreement with the observed electrophysiological threshold (10^{-12} μmol/l). This confirms that the models and parameter values offer a satisfactory description of the experimental data, as pointed out by Kaissling (Kaissling, 1998b). Two remarks must be added at this point. First, the definition of the dynamic range used here must not be interpreted as measuring the true dynamic range of the system studied. It is merely a convenient measure of the shape of the curve which removes the subjectivity of appreciating at which points the asymptotes are reached and permits one to compare responses of different systems. Second, the calculation presented above for S equal to the picomolar concentration of C or C^* is only a first approximation because with such a small number of molecules in interaction the deterministic description on which the present paper is based is no longer valid and must be replaced by a stochastic description. We have started to develop such a description for the CD models (Lánský and Rospars, 1993, 1995) and will extend these results in the future.

Odorant molecules released from a point source are carried away by the wind. The odorant plume formed is distorted by atmospheric turbulence and the concentration at a stationary point has been found to fluctuate at a frequency of some tens of cycles per second (Murlis *et al.*, 1992). Flying insects use this fluctuation to orient towards an odor source (Kramer, 1986). Successful orientation and source location is elicited in moths at frequencies of 2–10 s^{-1} (Vickers and Baker, 1992). Olfactory receptor neurons in *A. polyphemus* were shown to follow trains of short pulses (20 ms) at relatively high concentration (2.5×10^{-9} μmol/l) up to 0.5 and 10 s^{-1} depending on the neuron type (Christensen and Hildebrand, 1988; Rumbo and Kaissling, 1989; Marion-Poll and Tobin, 1992). The model studied is in

remarkable agreement with these data. Our numerical simulations (Figure 9) show that in the critical region (1–10 Hz) the amplitude of the periodic part of the signaling-complex response falls from 75 to 2% of the mean amplitude. For higher frequencies, which are accompanied by a larger amount of odorant delivered, the periodic part is practically smoothed out.

Acknowledgements

References

Ache, B.W. (1994) *Towards a common strategy for transducing olfactory information*. Semin. Cell Biol., 5, 55–63.

Beidler, B.W. (1962) *Taste receptor stimulation*. Prog. Biophys. Chem., 12,107–151.

Buck, L. (1996) *Information coding in the vertebrate olfactory system*. Annu. Rev. Neurosci., 19, 517–544.

Christensen, T.C. and **Hildebrand, J.G.** (1988) *Frequency coding by central olfactory neurons in the sphinx moth* Manduca sexta. Chem. Senses, 13, 123–130.

Ennis, D.M. (1991) *Molecular mixture models based on competitive and noncompetitive agonism*. Chem. Senses, 16, 1–17.

Getz, W.M. (1999) *A kinetic model of the transient phase in the response of olfactory receptor neurons*. Chem. Senses, 24, 497–508.

Getz, W.M. and **Akers, R.P.** (1995) *Partitioning non-linearities in the response of olfactory neurons to binary odors*. BioSystems, 34, 27–40.

Gnatzy, W., Mohren, W. and **Steinbrecht, R.A.** (1984) *Pheromone receptors in* Bombyx mori *and* Antheraea pernyi. *II. Morphometric analysis*. Cell Tissue Res., 235, 35–42.

Hildebrand, J.G. and **Shepherd, G.M.** (1997) *Mechanisms of olfactory discrimination: converging evidence for common principles across phyla*. Annu. Rev. Neurosci., 20, 595–631.

Kaissling, K.-E. (1969) *Kinetics of olfactory receptor potentials*. In Pfaffman, C. (ed.), Olfaction and Taste III. Rockefeller University Press, New York, pp. 52–70.

Kaissling, K.-E. (1971) *Insect olfaction*. In Beidler, L.M. (ed.), Handbook of Sensory Physiology. Springer, Berlin, pp. 351–431.

Kaissling, K.-E. (1974) *Sensory transduction in insect olfactory receptors*. In Jaenicke, L. (ed.), Biochemistry of Sensory Functions. Springer, Berlin, pp. 243–273.

Kaissling, K.-E. (1986) *Chemo-electrical transduction in insect olfactory receptors*. Annu. Rev. Neurosci., 9, 121–145.

Kaissling, K.-E. (1987) In Colbow, K. (ed.) R.H. Wright Lectures on Insect Olfaction. Simon Fraser University, Burnaby, pp. 1–190.

Kaissling, K.-E. (1995) *Single unit and electroantennogram recordings in insect olfactory organs*. In Spielman, A.I., and Brand, J.G. (eds), Experimental Cell Biology of Taste and Olfaction: Current Techniques and Protocols. CRC Press, Boca Raton, FL, pp. 361–386.

Kaissling, K.-E. (1996) *Peripheral mechanisms of pheromone reception in moths*. Chem. Senses, 21, 257–268.

Kaissling, K.-E. (1998a) *Flux detectors vs. concentration detectors: two types of chemoreceptors*. Chem. Senses, 23, 99–111.

Kaissling, K.-E. (1998b) *Pheromone deactivation catalyzed by receptor molecules: a quantitative kinetic model*. Chem. Senses, 23, 385–395.

Kaissling, K.-E. and **Priesner, E.** (1970) *Die Riechschwelle des Seidenspinners*. Naturwissenschaften, 57, 23–28.

Kanaujia, S. and **Kaissling, K.-E.** (1985) *Interactions of pheromone with moth antennae: adsorption, desorption and transport*. J. Insect Physiol., 31, 71–81.

Kasang, G., von Proff L. and **Nicholls M.** (1988) *Enzymatic conversion and degradation of sex pheromones in antennae of the male silkworm moth* Antheraea polyphemus. Z. Naturforsch., 43c, 275–284.

Keil, T.A. (1984) *Reconstruction and morphometry of silkmoth olfactory hairs: a comparative study of sensilla trichodea on the antennae of male* Anthereaea polyphemus *and* Antheraea pernyi *(Insecta, Lepidoptera)*. Zoomorphology, 104, 147–156.

Kennedy, J.S., Ludlow, A.R. and **Sanders, C.J.** (1980) *Guidance system used in moth sex attraction*. Nature, 288, 474–477.

Kramer, E. (1986) *Turbulent diffusion and pheromone-triggered anemotaxis*. In Payne, T.L., Birch, M.C. and Kennedy, C.E.J. (eds), Mechanisms in Insect Olfaction. Clarendon Press, Oxford, pp. 59–67.

Lancet, D. and **Ben-Arie, N.** (1993) *Olfactory receptors*. Curr. Biol., 3, 329–355.

Lánský, P. and **Rospars, J.-P.** (1993) *Coding of odor intensity*. BioSystems, 31, 15–38.

Lánský, P. and **Rospars, J.-P.** (1995) *Mathematical approach to transduction processes in olfactory receptor neurons*. J. Jap. Soc. Instrum. Control Eng., 34, 800–804.

Lánský, P. and **Rospars, J.-P.** (1998) *Odorant concentration and receptor potential in olfactory sensory neurons*. BioSystems, 48, 131–138.

Lasareff, P. (1922) *Untersuchungen über die Ionentheorie der Reizung. III. Mitteilung. Ionentheorie de Geschmacksreizung*. Arch. Ges. Physiol., 194, 293–297.

Lauffenburger, D.A. and **Linderman, J.** (1993) Receptors, Models for Binding, Trafficking, and Signaling. Oxford University Press, Oxford.

Malaka, R., Ragg, T. and **Hammer, M.** (1995) *Kinetic models of odor transduction implemented as artificial neural networks*. Biol. Cybern., 73, 195–207.

Marion-Poll, F. and **Tobin, T.R.** (1992) *Temporal coding of pheromone pulses and trains in* Manduca sexta. J. Comp. Physiol. A, 171, 505–512.

Meng, L.Z., Wu, C.H., Wicklein, M. and **Kaissling, K.-E.** (1989) *Number and sensitivity of three types of pheromone receptor cells in* Antheraea pernyi *and* A. polyphemus. J. Comp. Physiol. A, 165, 139–146.

Murlis, J. (1997) *Odor plumes and the signal they provide*. In Cardé, R.T. and Minks, A.K. (eds), Insect Pheromone Research: New Directions. Chapman & Hall, New York, pp. 221–231.

Murlis, J.S., Elkinton, J.S. and **Cardé, R.T.** (1992) *Odor plumes and how insects use them*. Annu. Rev. Entomol., 37, 505–532.

Pelosi, P. (1996) *Perireceptor events in olfaction*. J. Neurobiol., 30, 3–19.

Ronnett, G.V. and **Snyder, S.H.** (1992) *Molecular messengers of olfaction*. Trends Neurosci., 15, 508–513.

Rospars, J.-P., Lánský, P. and **Fort, J.-C.** (1996a) *Modelling odor intensity and odor quality coding in olfactory systems*. In Torre, V. and Conti, F. (eds), Neurobiology: Ionic Channels, Neurons, and the Brain. Plenum, New York, pp. 217–231.

Rospars, J.-P., Lánský, P., Tuckwell, H.C. and **Vermeulen, A.** (1996b) *Coding of odor intensity in a steady-state deterministic model of an olfactory receptor neuron*. J. Comput. Neurosci., 3, 51–72.

Rospars, J.-P., Lansky, P., Duchamp-Viret and **Duchamp, A.** (2000) *Spiking frequency vs. odorant concentration in olfactory receptor neurons*. BioSystems (in press).

Rumbo, E.R. and **Kaissling, K.-E.** (1989) *Temporal resolution of odour pulses by three types of pheromone receptor cells in* Antheraea polyphemus. J. Comp. Physiol. A, 165, 281–291.

Schild, D. and **Restrepo, D.** (1998) *Transduction mechanisms in vertebrate olfactory receptor cells*. Physiol. Rev., 78, 429–466.

Shepherd, G.M. (1992) *Discrimination of molecular signals by the olfactory receptor neuron*. Neuron, 13, 771–790.

Stange, G. (1996) *Sensory and behavioural responses of terrestrial invertebrates to biogenic carbon dioxide gradients*. In Stanhill, G. (ed.), Advances in Bioclimatology. Springer, Heidelberg, Vol. 4, pp. 223–253.

Tateda, H. (1967) *Sugar receptor and α-amino acid in the rat*. In Hayashi, T. (ed.), Olfaction and Taste II. Pergamon Press, Oxford, pp. 383–397.

Vermeulen, A. and **Rospars, J.-P.** (1998) *Dendritic integration in olfactory sensory neurons: a steady-state analysis of how the neuron structure and neuron environment influence the coding of odor intensity*. J. Comput. Neurosci., 5, 243–266.

Vickers, N.J. and **Baker, T.C.** (1992) *Male* Heliothis virescens *maintain upwind flight in response to experimentally pulsed filaments of their sex pheromone (Lepidoptera, Noctuidae)*. J. Insect Behav., 5, 699–687.

Willis, M.A. and **Baker, T.C.** (1984) *Effects of intermittent and continuous pheromone stimulation on the flight behavior of the oriental fruit moth,* Grapholita molesta. Physiol. Entomol., 9, 341–358.

Zack, C. (1979) Sensory Adaptation in the Sex Pheromone Receptor Cells of Saturniid Moths. Dissertation, Fakultät Biologie Ludwig-Maximilians-Universität, Munich.

Ziegelberger, G. (1995) *Redox-shift of the pheromone-binding protein in the silkmoth* Antheraea polyphemus. Eur. J. Biochem., 232, 706–711.

Appendix: differential equations

Using principles of mass action kinetics, the reactions for the six models studied, summarized in Table 1, can be readily translated into differential equations giving the time rate of change of the various chemical species of interest. In all models a relation of conservation for the total number N of receptors holds; in single-step models (CD1, FD1 and GFD1) the relation is

$$R(t) + C(t) = N$$

and in double-step models (CD2, FD2, GFD2) it is

$$R(t) + C(t) + C^*(t) = N$$

with N constant at any time. Due to these relations, the number of independent differential equations is decreased by one with respect to the number of chemical species (or states) involved.

Model CD1 (single step)

Only one independent equation can be written. We select the equation for C as it is the quantity of interest,

$$\frac{dC(t)}{dt} = -\left(k_{-1} + k_1 L_{ex}(t)\right)C(t) + k_1 L_{ex}(t)N \tag{A1}$$

If $L_{ex}(t)$ is small, i.e. $k_{-1} \gg k_1 L_{ex}(t)$, equation (A1) can be simplified into the form

$$\frac{dM(t)}{dt} = -k_{-1}M(t) + k_1 L_{ex}(t)N \tag{A2}$$

Model CD2 (double step)

Only two independent equations can be written,

$$\frac{dC(t)}{dt} = -\left(k_{-1} + k_1 L_{ex}(t) + k_2\right)C(t) + \left(k_{-2} - k_1 L_{ex}(t)\right)C^*(t) + k_1 L_{ex}(t)N \tag{A3}$$

and

$$\frac{dC^*(t)}{dt} = -k_{-2}C^*(t) + k_2 C(t) \tag{A4}$$

If $L_{ex}(t)$ is small, i.e. k_{-1} and now additionally k_{-2} prevail over $k_1 L_{ex}(t)$, formally when $k_{-1} \gg k_1 Lex(t)$ and $k_{-2} \gg k_1 L_{ex}(t)$, equation (A3) becomes

$$\frac{dM(t)}{dt} = -\left(k_{-1} + k_2\right)M(t) + k_{-2}M^*(t) + k_1 L_{ex}(t)N \tag{A5}$$

whereas equation (A4) remains unchanged (only with different notation),

$$\frac{dM^*(t)}{dt} = -k_{-2}M^*(t) + k_2 M(t) \tag{A6}$$

The conditions leading to equation (A5) imply that the number of interacting receptors is far below their total number, $C(t) + C^*(t) \ll N$. Again, the external stimulation appears in equation (A5) as an additive term only.

Model FD1 (single step)

The system can be described by two independent equations, e.g.

$$\frac{dC(t)}{dt} = -\left(k_{-1} + k_o + k_1 L(t)\right)C(t) + k_1 L(t)N \tag{A7}$$

$$\frac{dL(t)}{dt} = k_i L_{ex}(t) - k_1 L(t)N + \left(k_1 L(t) + k_{-1}\right)C(t) \tag{A8}$$

If $k_i L_{ex}(t) << k_o$, which implies $C(t) << N$, then equations (A7) and (A8) can be reduced to a simpler system

$$\frac{dM(t)}{dt} = -(k_{-1} + k_o)M(t) + k_1 L^M(t)N \qquad (A9)$$

$$\frac{dL^M(t)}{dt} = k_i L_{ex}(t) - k_1 L^M(t)N + k_{-1}M(t) \qquad (A10)$$

where the upper index in $L^M(t)$ makes the distinction from $L(t)$ in the complete model. The system of equations (A9) and (A10) is formally the same as that of equations (A5) and (A6), but with different interpretation of the parameters.

Model FD2 (double step)

Three independent equations can be written

$$\frac{dL(t)}{dt} = k_i L_{ex}(t) - k_1 L(t)(N - C(t) - C^*(t)) + k_{-1}C(t) \qquad (A11)$$

$$\frac{dC(t)}{dt} = -(k_{-1} + k_2)C(t) + k_1 L(t)(N - C(t) - C^*(t)) + k_{-2}C^*(t) \qquad (A12)$$

$$\frac{dC^*(t)}{dt} = -(k_{-2} + k_o)C^*(t) + k_2 C(t) \qquad (A13)$$

If the number of interacting receptors $C(t) + C^*(t)$ is sufficiently small compared with N, then equations (A11)–(A13) simplifies to

$$\frac{dL^M(t)}{dt} = k_i L_{ex}(t) - k_1 L^M(t)N + k_{-1}M(t) \qquad (A14)$$

$$\frac{dM(t)}{dt} = -(k_{-1} + k_2)M(t) + k_1 L^M(t)N + k_{-2}M^*(t) \qquad (A15)$$

$$\frac{dM^*(t)}{dt} = -(k_{-2} + k_o)M^*(t) + k_2 M(t) \qquad (A16)$$

Model GFD1 (single step)

Only two independent equations can be considered, (A7) and

$$\frac{dL(t)}{dt} = \max(0, k_i L_{ex}(t) - k_{-1}L(t)) - k_1 L(t)N + (k_1 L(t) + k_{-1})C(t) \qquad (A17)$$

If $C(t) << N$, which is again equivalent to $k_i L_{ex} << k_o$, the simplified system is formed by equation (A9) and

$$\frac{dL^M(t)}{dt} = \max(0, k_i L_{ex}(t) - k_{-i}L^M(t)) - k_1 L^M(t)N + k_{-1}M(t) \qquad (A18)$$

Model GFD2 (double step)

This model is described by equations (A12), (A13) and

$$\frac{dL(t)}{dt} = \max(0, k_i L_{ex}(t) - k_{-1}L(t)) - k_1 L(t)(N - C(t) - C^*(t)) + k_{-1}C(t) \qquad (A19)$$

and for the simplified situation it is defined by equations (A15), (A16) and

$$\frac{dL^M(t)}{dt} = \max(0, k_i L_{ex}(t) - k_{-i}L^M(t)) - k_1 L^M(t)N + k_{-1}M(t) \qquad (A20)$$